

Electronic Supplementary Information for Molecular Insights: Structure and Dynamics of a Li Ion Doped Organic Ionic Plastic Crystal

Liyu Jin,^{†,‡} Simon de Leeuw,^{*,¶} Marina V. Koudriachova,[§] Jennifer M. Pringle,^{||,‡}
Patrick C. Howlett,^{||,‡} Fangfang Chen,^{||} and Maria Forsyth^{*,||,‡}

*Department of Materials Engineering, Monash University, Wellington Rd, Clayton VIC
3800, Australia, ARC Centre of Excellence for Electromaterials Science, Theoretical
Chemistry, Gorlaeus Laboratories, Leiden University, Einsteinweg 55, 2333 CC Leiden,
The Netherlands, Department of Chemistry, University College London, Gower Street,
London WC1E 6BT, United Kingdom, and Institute for Frontier Materials, Deakin
University, 221 Burwood Highway, Burwood VIC 3125, Australia*

E-mail: leeuwdes@chem.leidenuniv.nl; maria.forsyth@deakin.edu.au

*To whom correspondence should be addressed

[†]Monash University

[‡]ARC Centre of Excellence for Electromaterials Science

[¶]Leiden University

[§]University College London

^{||}Deakin University

Computational Details

The unit cell of tetramethylammonium dicyanamide ([TMA][DCA]) obtained from a single crystal X-ray diffraction experiment was used to construct the simulation "supercell". It consists of $4 \times 2 \times 2 = 16$ unit cells, containing 128 ion pairs. To create the structures of doped [TMA][DCA] with various concentrations of LiDCA, 5, 10 or 15 Li⁺s replaced the equivalent number of [TMA]⁺ in 4, 8 or 12 mol% systems, respectively. (It was checked that scaling of the "supercell" size up to $8 \times 4 \times 4 = 128$ unit cells, with corresponding scaling of Li⁺ numbers (to keep the same concentrations) did not make any noticeable difference in terms of structural and dynamics results.) The inserted Li⁺ took the coordinates of the original central nitrogens' of the replaced [TMA]⁺s. The replaced [TMA]⁺s were selected "randomly" by the internal Matlab[®] algorithm *rand*. It is worth noting that we tested three different configurations with the same Li⁺ concentration but totally different Li⁺s' positions in the lattice. They gave us the same results (spatial correlation functions, time autocorrelation functions, *etc.*) All the molecular dynamic simulations were carried out using The DL_POLY Classic (v1.8) software package.¹ DL_FIELD (v2.1)² package was used to convert structural information of the manipulated "supercells" to DL_POLY recognized CONFIG files. The NPT ensemble was applied using Berendsen thermostat and barostat to keep the systems at constant temperatures and pressures with the relaxation time of 1 ps. The systems were equilibrated for 500 ps using a timestep of 2 fs (the equilibration states were reached, which was confirmed by the convergence of temperature, total energy, volume and pressure) followed by a production run of 500 ps for data collection.

All the force field parameters for this particular ion pair described below were developed by Adebahr *et.al.*³ For the internal degrees of freedom, bond stretching and angle bending, harmonic potentials were taken and the parameters are listed in Table S1 and S2. It is noteworthy that the methyl groups of the tetramethylammonium cations are only hindered intermolecularly by other methyl groups, since no bonded dihedral potentials were included. The Van der Waals forces were calculated by the Lennard-Jones potential model (the cutoff

set to 8.5 Å) with the parameters listed in Table S3. To calculate the parameters for unlike atoms, the Lorentz-Berthelot combining rule were adopted ($\epsilon_{ij} = \sqrt{\epsilon_{ii}\epsilon_{jj}}$ and $\sigma_{ij} = (\sigma_{ii} + \sigma_{jj})/2$). The electrostatic potentials are calculated by the Ewald Sum method with Ewald precision set to $1.0E - 6$, and partial charges on each atoms listed in Table S3.

Table S1: Harmonic bond potential parameters ($U(r) = \frac{1}{2}K(r - r_0)^2$), **K** is force constant and r_0 is equilibrium length

Bond	r_0 (Å)	K(kcal mol ⁻¹ Å ⁻²)
C-H ([TMA])	0.9931	771
C-N ([TMA])	1.4987	719
N-C (central N, [DCA])	1.3120	1278
C-N (terminal N, [DCA])	1.1539	2075

Table S2: Harmonic angle potential parameters ($U(\theta) = \frac{1}{2}K(\theta - \theta_0)^2$), **K** is force constant and θ_0 is equilibrium angle

Angle	θ_0 (°)	K(kcal mol ⁻¹ rad ⁻²)
C-N-C ([TMA])	109.47	158
N-C-H ([TMA])	107.21	111
H-C-H ([TMA])	111.74	73
C-N-C ([DCA])	120.71	70
N-C≡N ([DCA])	173.25	93

Table S3: Intermolecular interaction potential parameters, van der Waals potentials (Lennard-Jones: $U(r) = 4\epsilon((\frac{\sigma}{r})^{12} - (\frac{\sigma}{r})^6)$ and electrostatic potentials (Ewald Sum))

Atom	Charge	σ (Å)	ϵ (kcal mol ⁻¹)
C ([TMA])	-0.277	3.87	0.02
H ([TMA])	+0.16	2.48	0.0055
N ([TMA])	+0.188	3.48	0.05
N (central nitrogen [DCA])	-0.7017	3.48	0.05
C ([DCA])	+0.5797	3.39	0.0225
N (terminal nitrogen [DCA])	-0.7288	3.48	0.05
Li ⁺ (ref 4)	+1.0	2.96	0.022

Ionic Conductivity Calculation

The simulated ionic conductivities were calculated based on the Einstein model as shown in Equation S1:

$$\begin{aligned}\lambda_{DC} &= \lim_{t \rightarrow \infty} \lambda(t) = \frac{e^2}{6Vk_B T} \lim_{t \rightarrow \infty} \frac{\sum_{i=1}^N \sum_{j=1}^N z_i z_j \langle (\vec{r}_i(t) - \vec{r}_i(0)) \cdot (\vec{r}_j(t) - \vec{r}_j(0)) \rangle}{t} \\ &= \frac{e^2}{6Vk_B T} \lim_{t \rightarrow \infty} \frac{\langle (\sum_{i=1}^N z_i \vec{r}_i(t) - \sum_{i=1}^N z_i \vec{r}_i(0))^2 \rangle}{t}\end{aligned}\quad (1)$$

and

$$\sum_{i=1}^N z_i \vec{r}_i(t) = \sum_{i=1}^{N_c} z_i \vec{r}_i(t) - \sum_{i=1}^{N_a} z_i \vec{r}_i(t)$$

where λ_{DC} is the equilibrium DC conductivity, e is the electron charge, t is time, V is the volume of the simulation box, k_B is Boltzmann's constant, T is the temperature, z_i is the charges of ion i in electrons, N is the number of all ions in the cell, $\vec{r}_i(t)$ is the position of particle i at time t , N_c or N_a are the number of the cation or anion in the system, respectively. The angled brackets means the ensemble average of the systems.

Relevant Data

Volume change as function of Li doping level

The volume expansion has observed as we increased the doping levels to 8 and 12 mol% at 400 K, which is consistent with our suggestion that "free volume" has been created by the observed clustering effect in the higher doping levels.

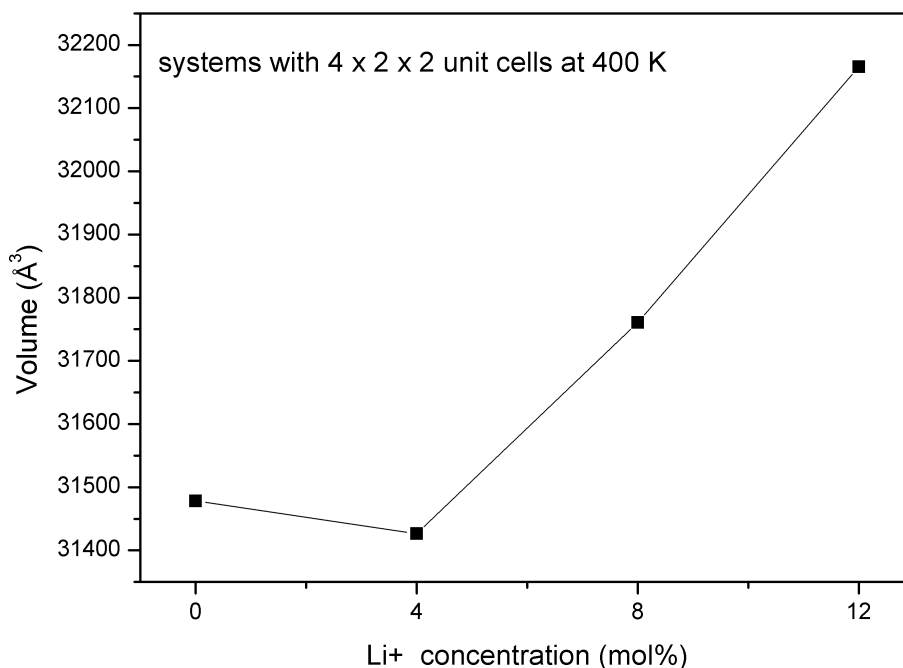


Figure S1: The volume expansion of simulated $4 \times 2 \times 2 = 16$ unit cells in 8 and 12 mol% Li ion doped systems due to "free volume" created by clustering effect. There is slight volume shrinkage in 4 mol% doped system. It suggests that with relative small amount of Li ions replacing TMA cations, the clustering effect is rather localized and the free volume created is insufficient to overcome the volume contraction due to much smaller physical radii (comparing to replaced TMA cations) of introduced Li ions.

Pure [TMA][DCA] systems

The simulations for pure systems can reproduce the results as shown in Ref 3, which is the starting point for further simulations of Li^+ doped systems. Moreover, by carefully sampling

the temperature range, we can differentiate three different phases (as described below), which helps in the analysis of doped systems.

Radial Distribution Functions (RDFs) of the Pure Systems

All these RDFs show three distinct regions:

1. From 200 K to 250 K, the peaks at different distances have higher intensity compared with those at other temperatures, and some peaks still can be observed up to 12.7Å, which is the end of RDF plot (limited by the minimum half-box-length). From those defined RDF peaks, it can be deduced that [TMA][DCA] has a highly rigid crystalline structure at these two temperatures.
2. From 500 K to 600 K, these three lines (500 K, 550 K and 600 K) are almost overlapping in all cases and the broadest and smoothest contour manifest the melt state.
3. For 350 K and 400 K, which indicates the region of plastic crystal phase, they have similar profile: the peaks are smooth but clearly show more detailed structural information than those above 500 K.

The other two temperature curves (300 K and 450 K) have similar features as their neighboring temperatures, indicating that they are probably in the transition states (from rigid crystal phase to plastic crystal phase and from plastic crystal phase to melt, respectively.)

More importantly, by referring to the experimental data (DSC),⁵ these simulation results are very well supported. As from the literature, the plastic crystal phase is from 380K to 450K and the structure melts at 450K, which are consistent with these RDF results.

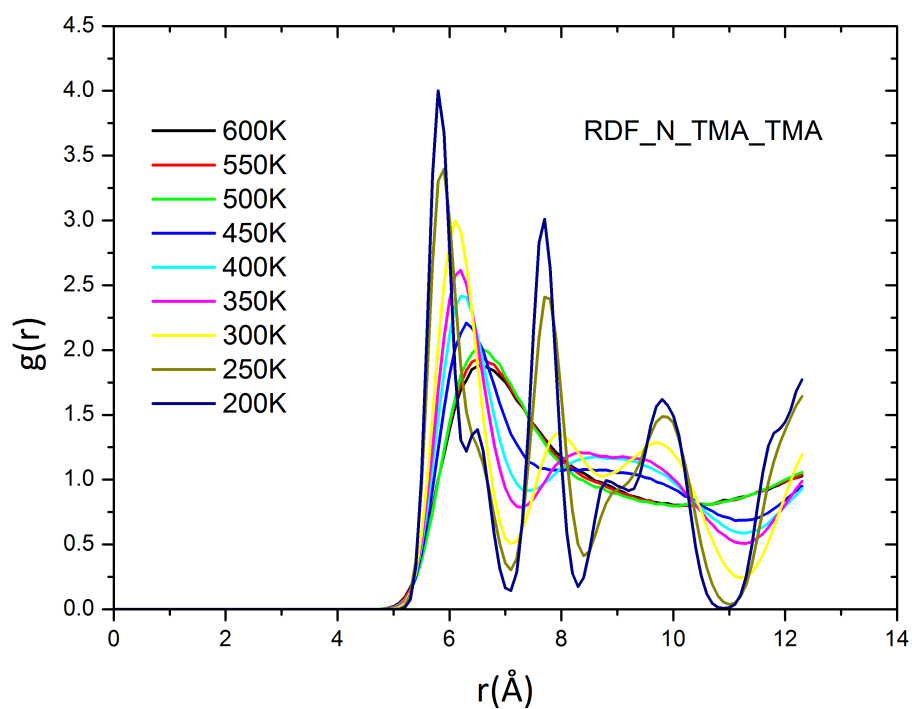


Figure S2: The RDFs of the central nitrogens of [TMA] vary as a function of temperature in the pure system. There are three distinctive phases, *i.e.* rigid crystal phase (200 and 250 K), plastic crystal phase (350 and 400 K) and melting phase (500 and 600 K).

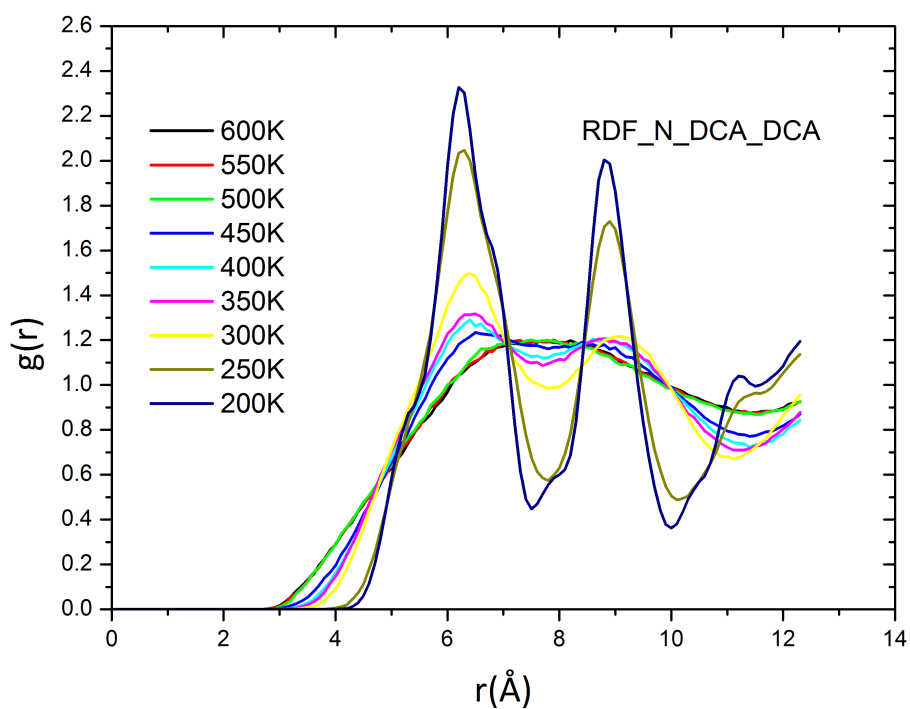


Figure S3: The RDFs of the central nitrogens of [DCA] vary as a function of temperature in pure the system. There are three distinctive phases, *i.e.* rigid crystal phase (200 and 250 K), plastic crystal phase (350 and 400 K) and melting phase (500 and 600 K).

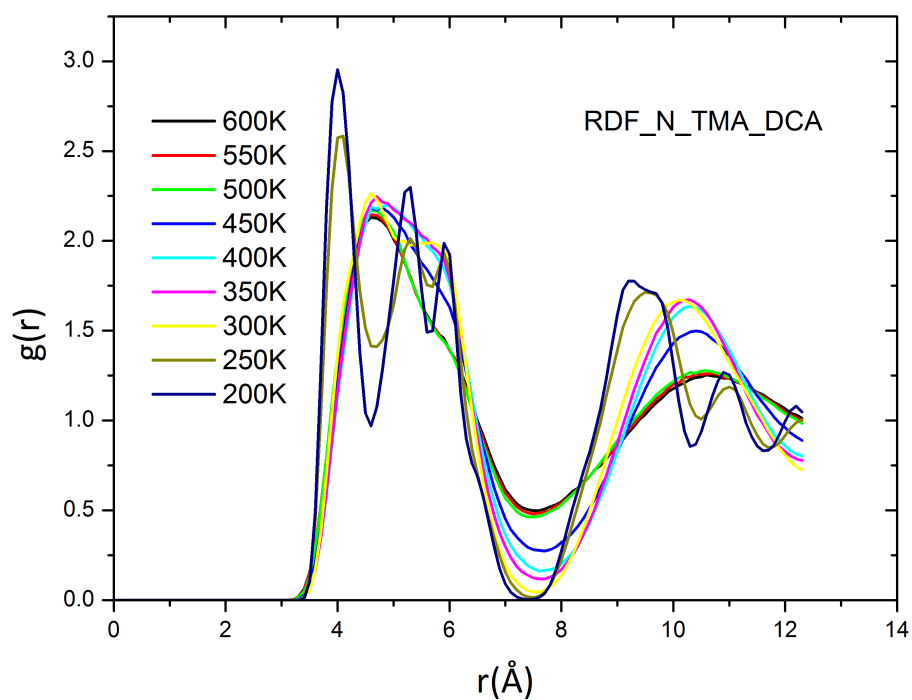


Figure S4: The RDFs of the central nitrogens between [TMA] and [DCA] vary as a function of temperature in the pure system. There are three distinctive phases, *i.e.* rigid crystal phase (200 and 250 K), plastic crystal phase (350 and 400 K) and melting phase (500 and 600 K).

Orientational Correlation of the Anions of the Pure Systems

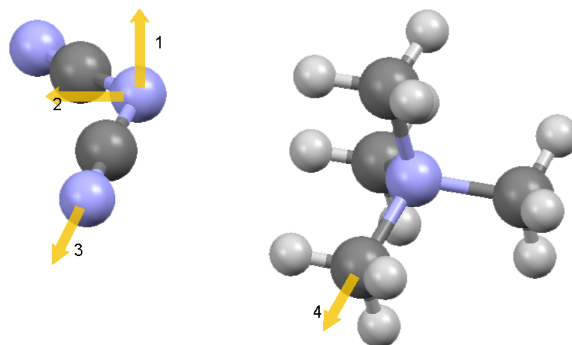


Figure S5: The vectors that are used in orientation correlation and rotation time autocorrelation calculations. Vector 1, perpendicular to [DCA] plane, Vector 2, in the [DCA] plane and through the centre of mass, Vector 3, through the N-C bond of [DCA], and Vector 4 through the N-C bond of [TMA].

The orientations of two ions are quantified by the following terms:

$$\cos \theta_{ij} = \vec{u}_j \cdot \vec{u}_i \quad (2)$$

where \vec{u} is the unit vector either perpendicular to or on the planes of DCA molecules. The orientational correlation function $d(r)$ is then defined as an ensemble average of $\cos \theta_{ij}$ for pairs of molecules i, j separated by a distance r :

$$d(r) = \langle \cos \theta_{ij} \rangle_r = \langle \vec{u}_j \cdot \vec{u}_i \rangle_r \quad (3)$$

The function $d(r)$ is the first in a series of averages of *Legendre Polynomials* P_n . In general we can define:

$$d_n(r) = \langle P_n(\cos \theta_{ij}) \rangle_r \quad (4)$$

Thus $d_1(r) = d(r)$ and

$$d_2(r) = \frac{1}{2} \langle 3 \cos^2 \theta_{ij} - 1 \rangle_r \quad (5)$$

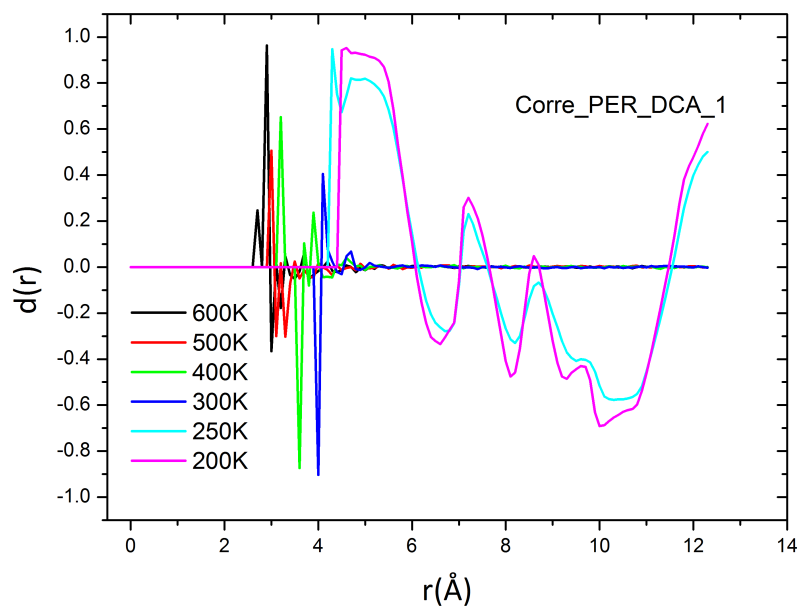


Figure S6: Correlations between the vectors normal to the DCA plane (Vector 1 in Figure S5, $d_1(r) = \langle \cos \theta \rangle_r$)

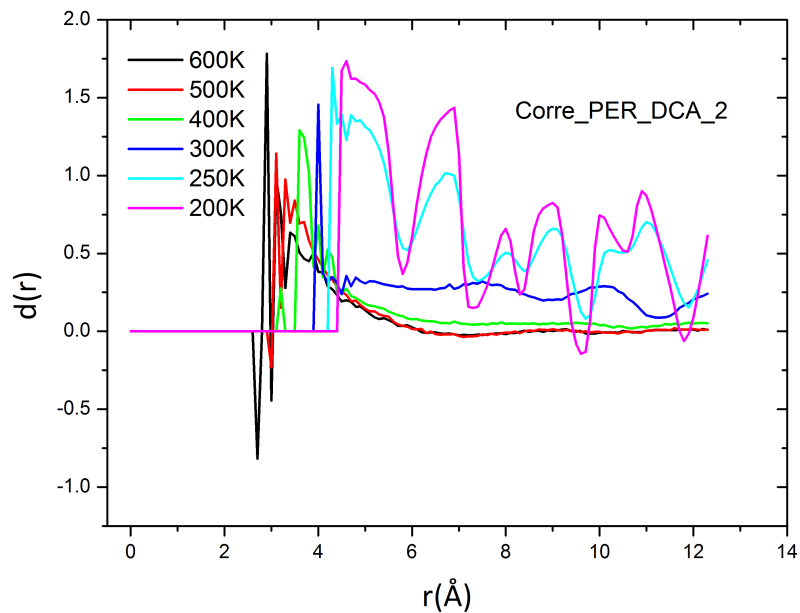


Figure S7: Correlations between the vectors normal to the DCA plane (Vector 1 in Figure S5, $d_2(r) = \frac{1}{2} \langle 3 \cos^2 \theta_{ij} - 1 \rangle_r$)

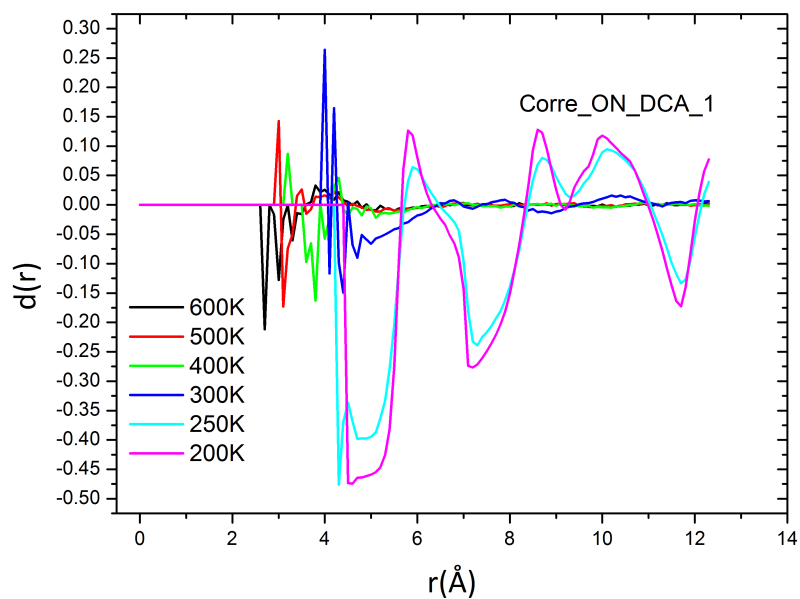


Figure S8: Correlations between the vectors in the DCA plane (Vector 2 in Figure S5, $d_1(r) = \langle \cos \theta \rangle_r$)

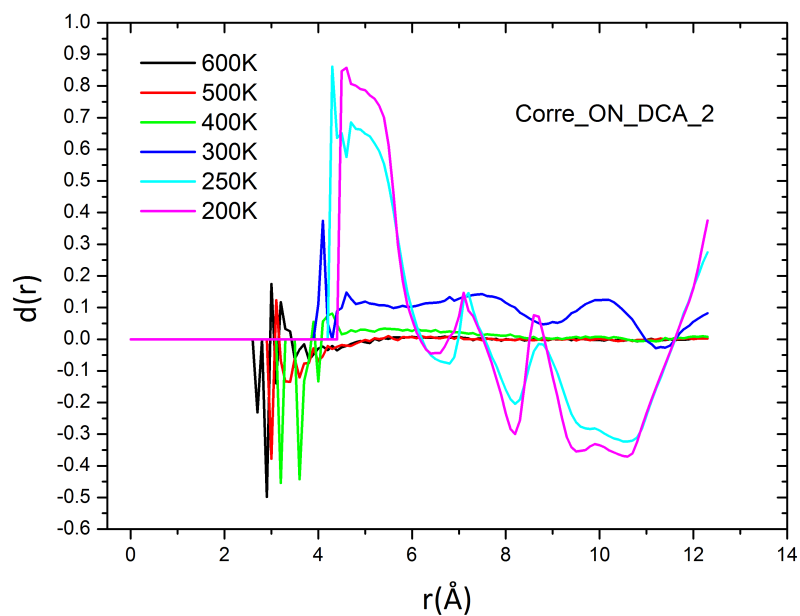


Figure S9: Correlations between the vectors in the DCA plane (Vector 2 in Figure S5, $d_2(r) = \frac{1}{2} \langle 3 \cos^2 \theta_{ij} - 1 \rangle_r$)

The C-N-C Angle of [DCA] Anions in the Pure Systems

The C-N-C angle of the [DCA]s do not show phase-dependent evolution, instead the anion gradually "opens up" as the temperature increases. This indicates that the plastic crystal behavior of this particular ion pair may be dominated by inter-molecular conformational changes (as shown by RDFs and orientational correlations) rather than the intra-molecular conformation change of the anions.

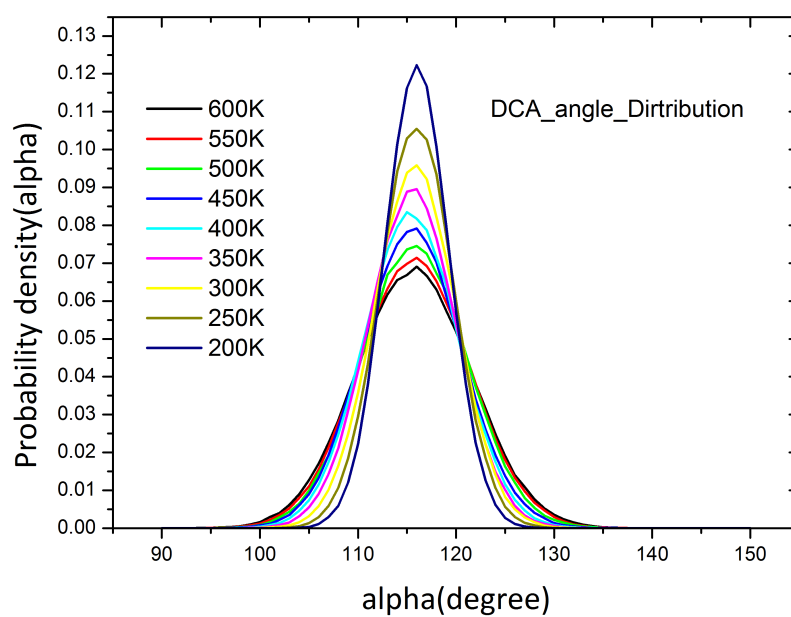


Figure S10: The ensemble average of C-N-C angle in the anion varies as a function of temperature in the pure system.

Rotational Time Autocorrelation Functions (RAFTs) of the Pure Systems

Rotational autocorrelation functions are consistent with the literature.³

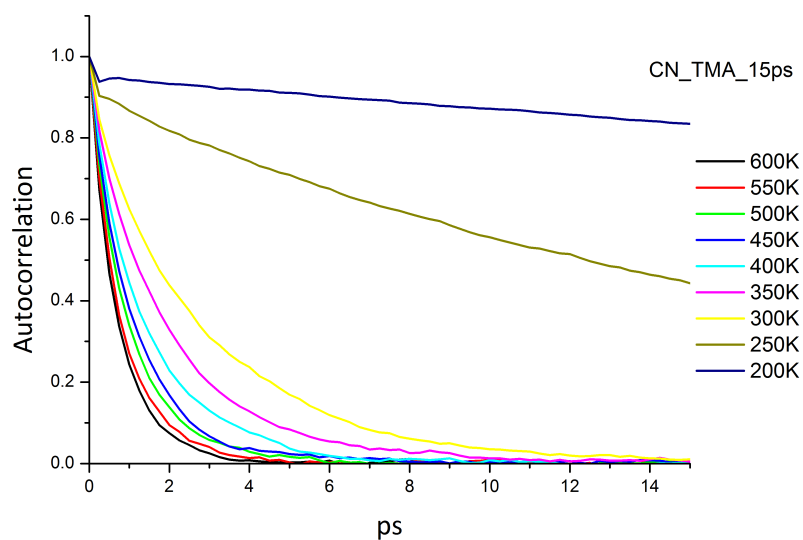


Figure S11: The rotational time autocorrelation function of C-N bond vector in TMA (Vector 4 in Figure S5.)

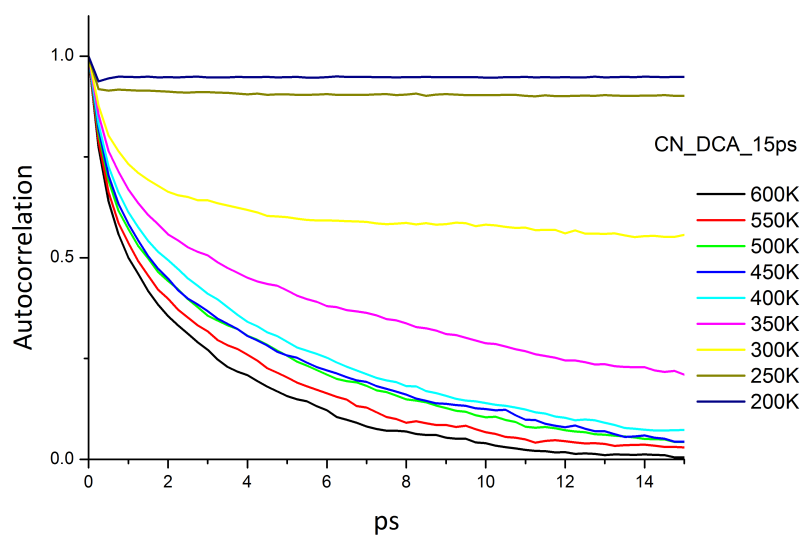


Figure S12: The rotational time autocorrelation function of C-N bond vector in the DCA (Vector 3 in Figure S5.)

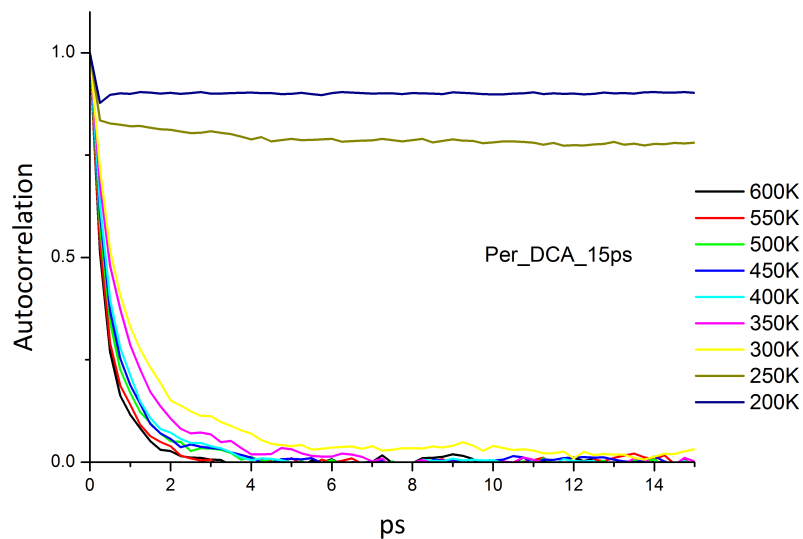


Figure S13: The rotational time autocorrelation function of the vector perpendicular to the DCA plane (Vector 1 in Figure S5.)

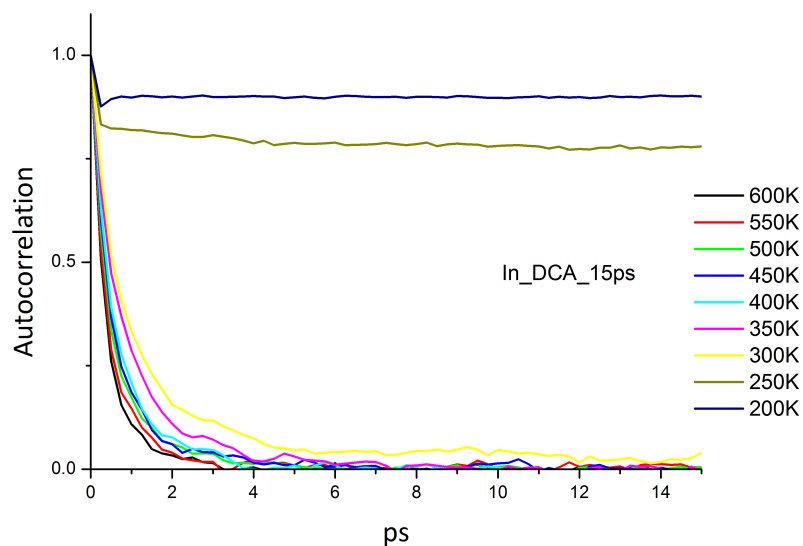


Figure S14: The rotational time autocorrelation function of the vector in DCA plane (Vector 2 in Figure S5.)

Mean Square Displacements (MSDs) of the Pure Systems

In the pure systems, the $\langle r^2 \rangle$ take off only above 450 K, which agrees well with experimental melting point (450 K).

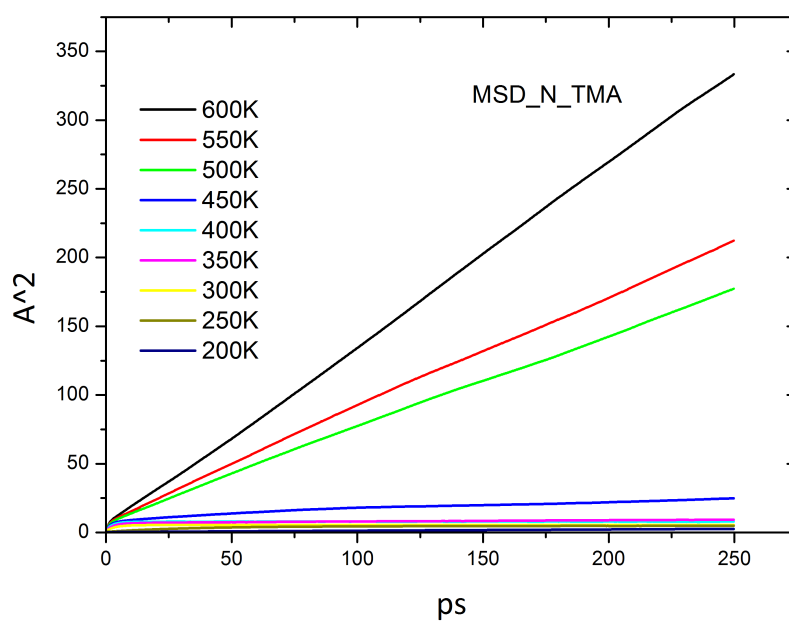


Figure S15: MSDs of the central Nitrogens of [TMA]s vary as a function of temperature in the pure system.

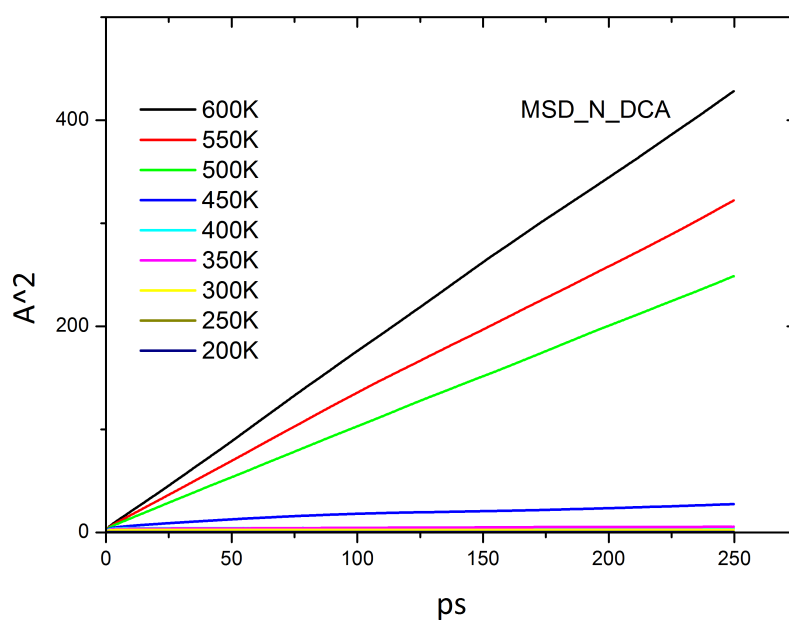


Figure S16: MSDs of the central Nitrogens of [DCA]s vary as a function of temperature in the pure system.

Li⁺ Doped [TMA][DCA] Systems

To clarify, the following figures use legends "+5Li", "+10Li" and "+15Li", which are equivalent to 4 mol%, 8 mol% and 12 mol% Li⁺ concentrations.

Radial Distribution Functions of the Li⁺ Doped Systems

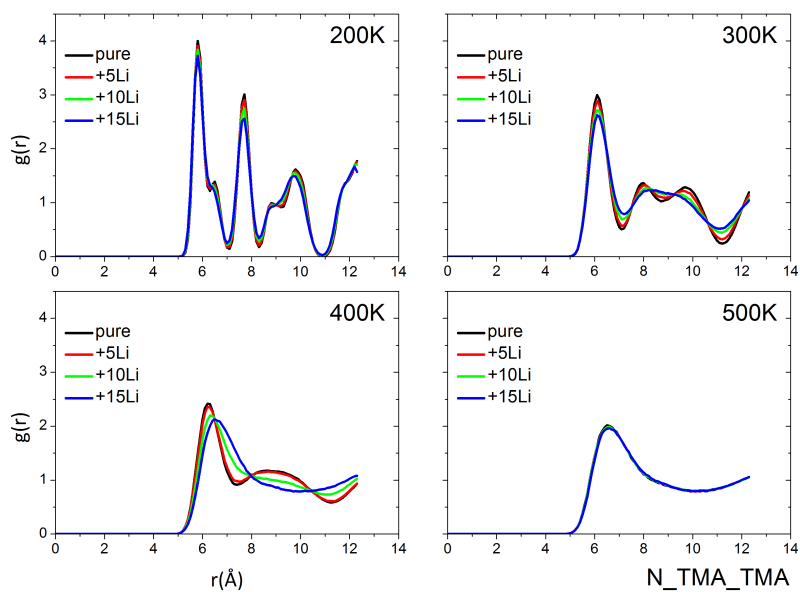


Figure S17: The RDFs (central nitrogens of cations) vary as a function of lithium doping level within four temperature regimes (200 K, 300 K, 400 K and 500 K)

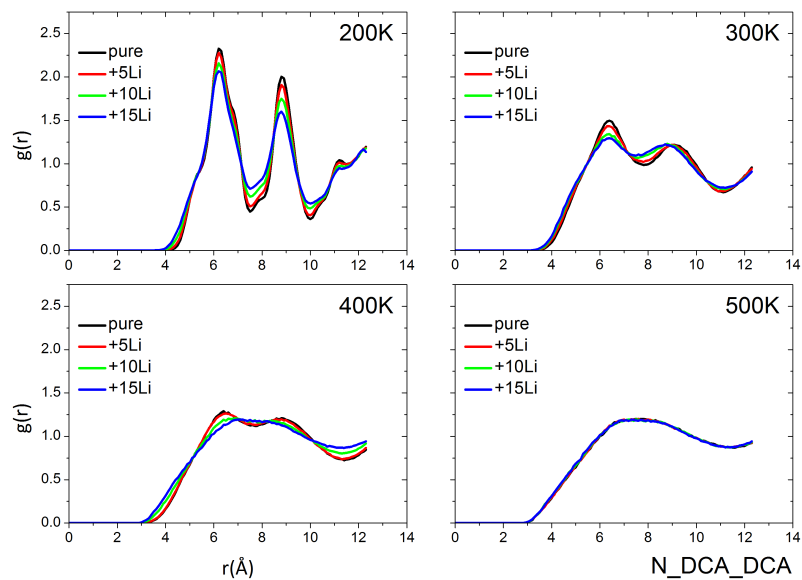


Figure S18: The RDFs (central nitrogens of anions) vary as a function of lithium doping level within four temperature regimes (200 K, 300 K, 400 K and 500 K)

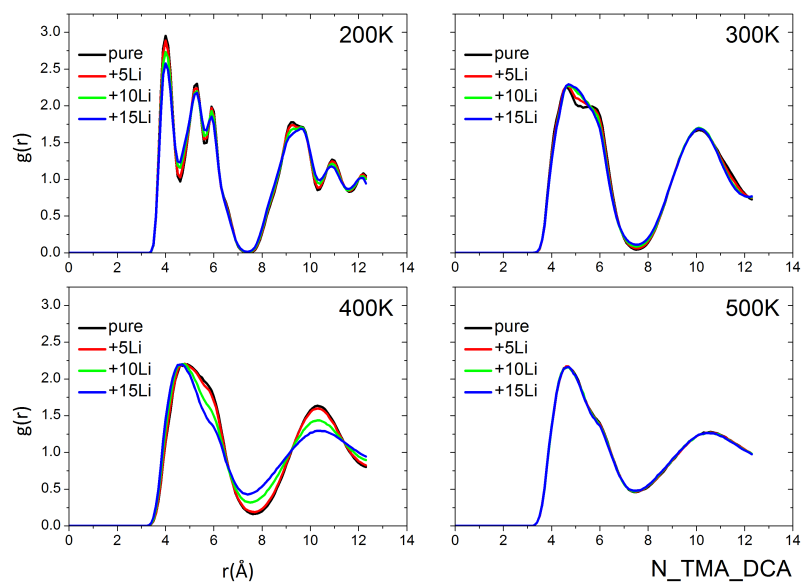


Figure S19: The RDFs (between central nitrogens of cations and anions) vary as a function of lithium doping level within four temperature regimes (200 K, 300 K, 400 K and 500 K).

Orientalional Correlation of the Anions of the Li⁺ Doped Systems

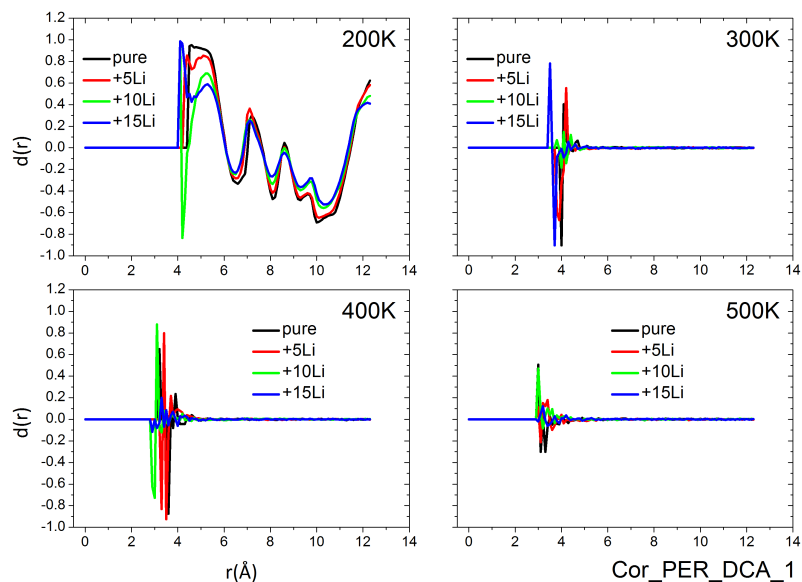


Figure S20: Correlations between the vectors normal to the DCA plane (Vector 1 in Figure S5, $d_1(r) = \langle \cos \theta \rangle_r$) vary as function of lithium doping level within four temperature regimes (200 K, 300 K, 400 K and 500 K).

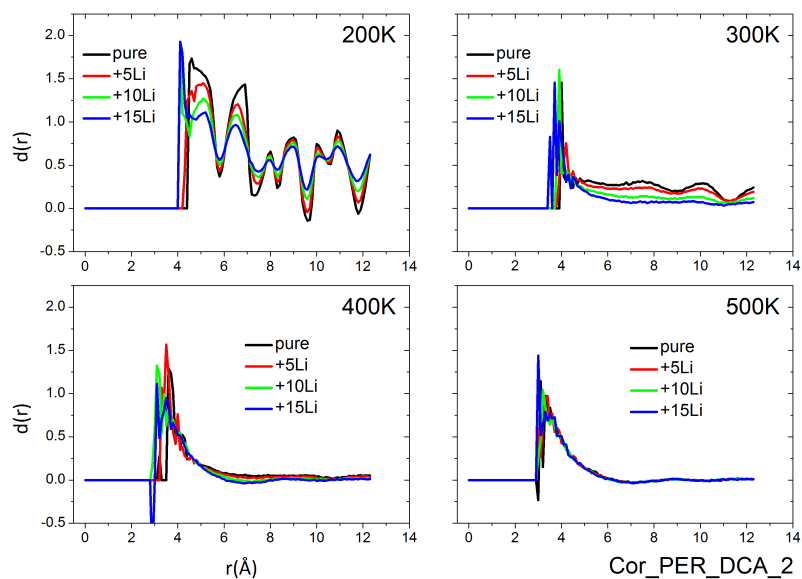


Figure S21: Correlations between the vectors normal to the DCA plane (Vector 1 in Figure S5, $d_2(r) = \frac{1}{2} \langle 3 \cos^2 \theta_{ij} - 1 \rangle_r$) vary as a function of lithium doping level within four temperature regimes (200 K, 300 K, 400 K and 500 K).

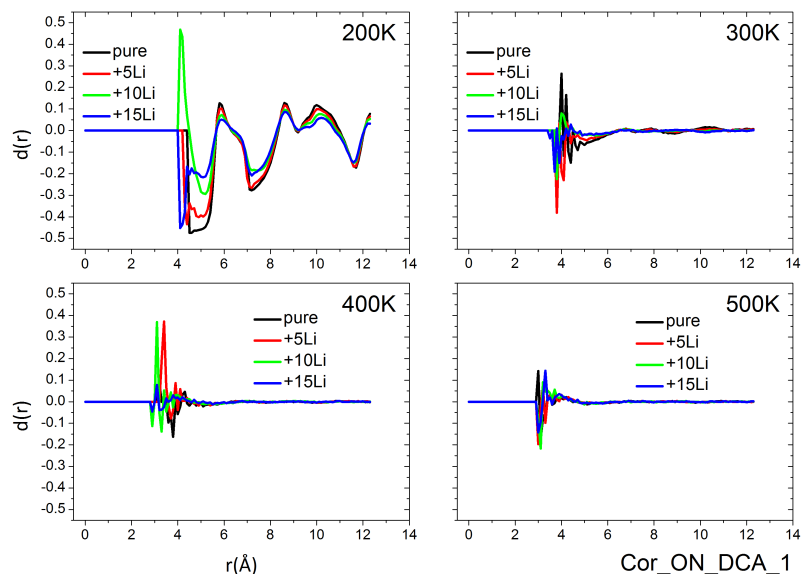


Figure S22: Correlations between the vectors in the DCA plane (Vector 2 in Figure S5, $d_1(r) = \langle \cos \theta \rangle_r$) vary as a function of lithium doping level within four temperature regimes (200 K, 300 K, 400 K and 500 K).

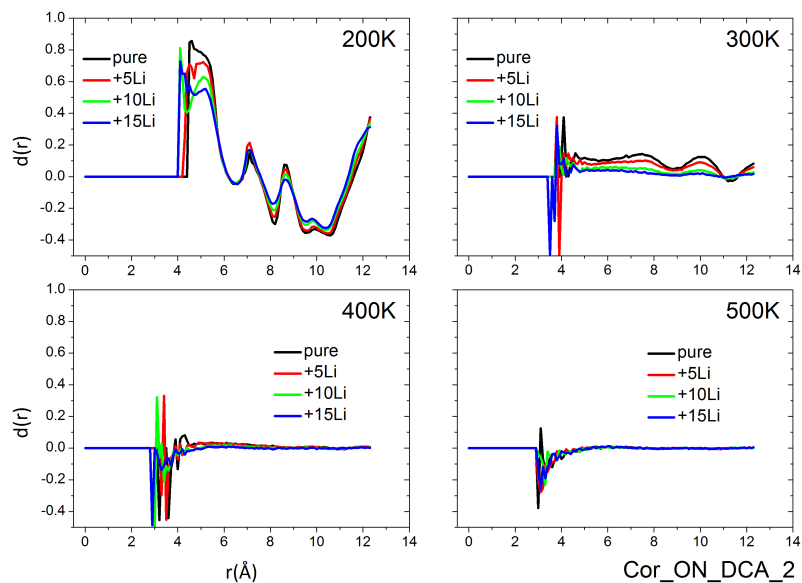


Figure S23: Correlations between the vectors in the DCA plane (Vector 2 in Figure S5, $d_2(r) = \frac{1}{2} \langle 3 \cos^2 \theta_{ij} - 1 \rangle_r$) vary as a function of lithium doping level within four temperature regimes (200 K, 300 K, 400 K and 500 K).

The C-N-C Angle of [DCA] anions in the Li⁺ Doped Systems

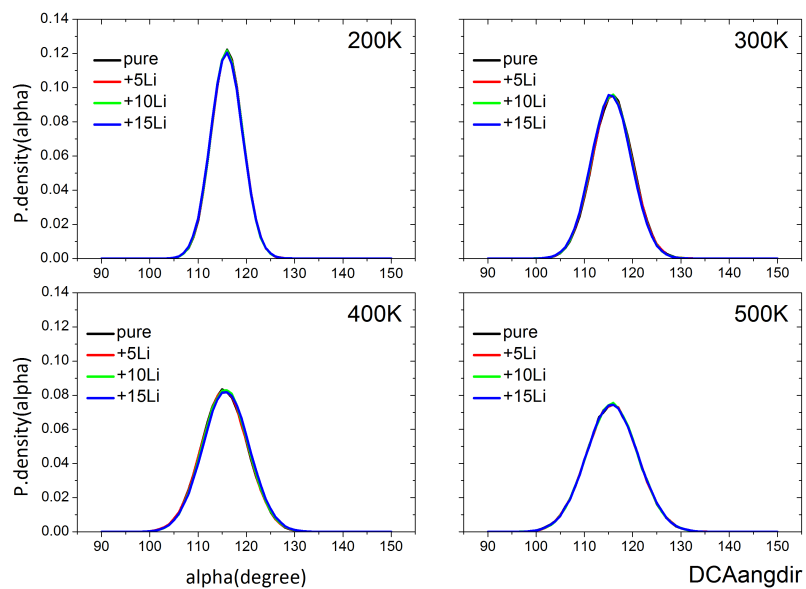


Figure S24: The ensemble average of C-N-C angles vary as a function of lithium doping level within four temperature regimes (200 K, 300 K, 400 K and 500 K).

Figure S24 shows that the doping of Li⁺ does not exert any effects on the C-N-C angles of [DCA]s, which are dominated by the thermal energy.

Rotational Time Autocorrelation Functions (RAFTs) of the Li^+ Doped Systems

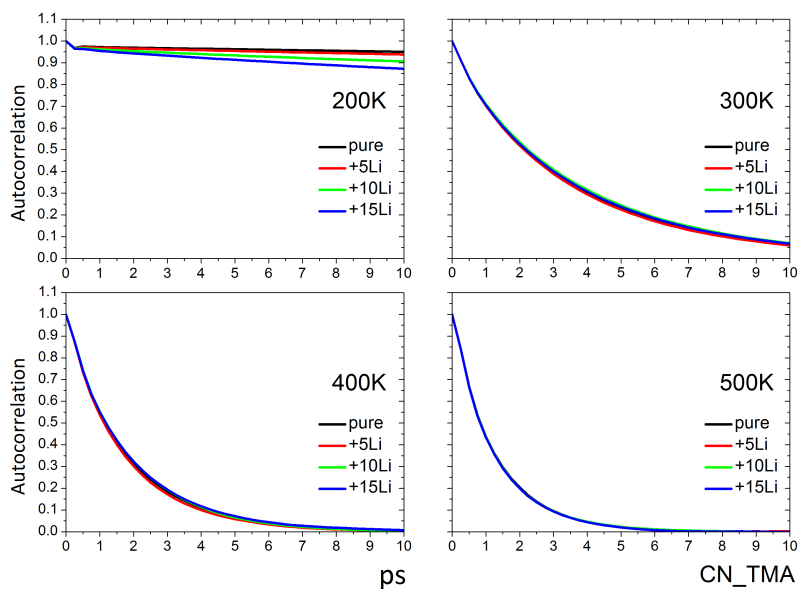


Figure S25: The rotational time autocorrelation function of C-N bond vector in TMA (Vector 4 in Figure S5.) varies as a function of the lithium doping level within four temperature regimes (200 K, 300 K, 400 K and 500 K).

Figure S25 shows that the doping of Li^+ does not exert remarkable effects on the rotational dynamics of [TMA]s in any phase. In contrast, the doped Li^+ s do affect the dynamics of [DCA]s (especially at 300 K and 400 K) as shown in Figure S26.

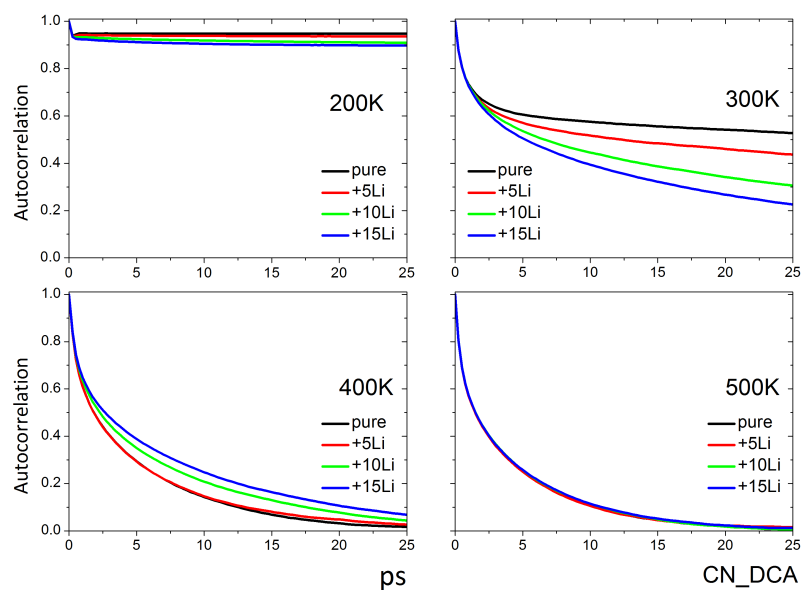


Figure S26: The rotational time autocorrelation function of the C-N bond vector in DCA (Vector 3 in Figure S5.) varies as a function of lithium doping level within four temperature regimes (200 K, 300 K, 400 K and 500 K).

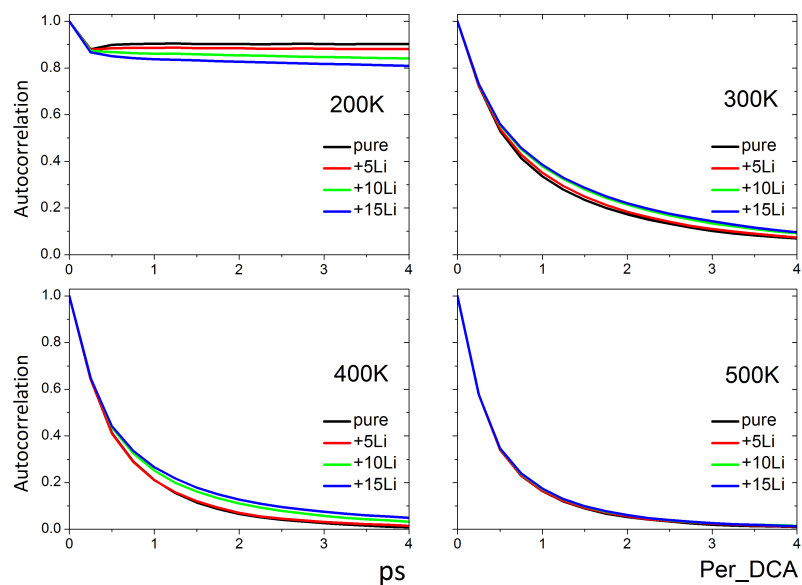


Figure S27: The rotational time autocorrelation function of the vector perpendicular to the DCA plane (Vector 1 in Figure S5.) varies as a function of lithium doping level within four temperature regimes (200 K, 300 K, 400 K and 500 K).

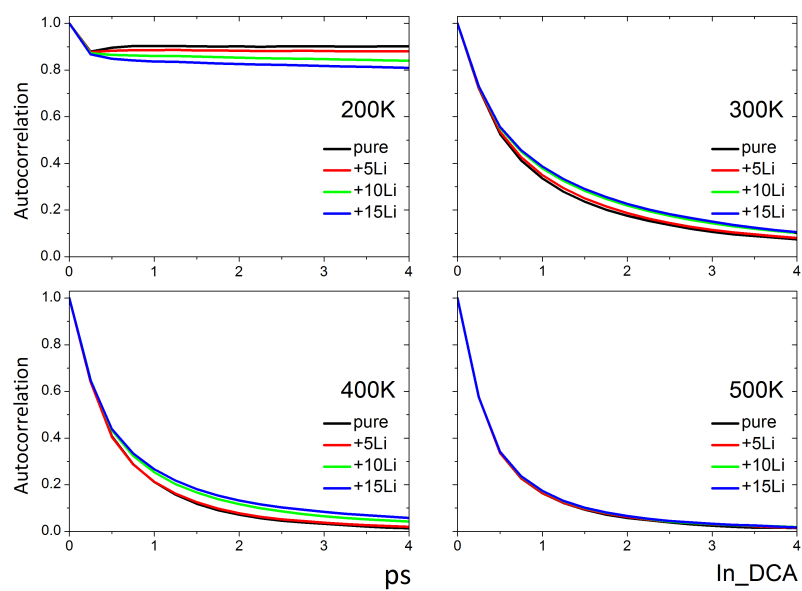


Figure S28: The rotational time autocorrelation function of the vector in the DCA plane (Vector 2 in Figure S5.) varies as a function of lithium doping level within four temperature regimes (200 K, 300 K, 400 K and 500 K).

Mean Square Displacements (MSDs) of the Li⁺ Doped Systems

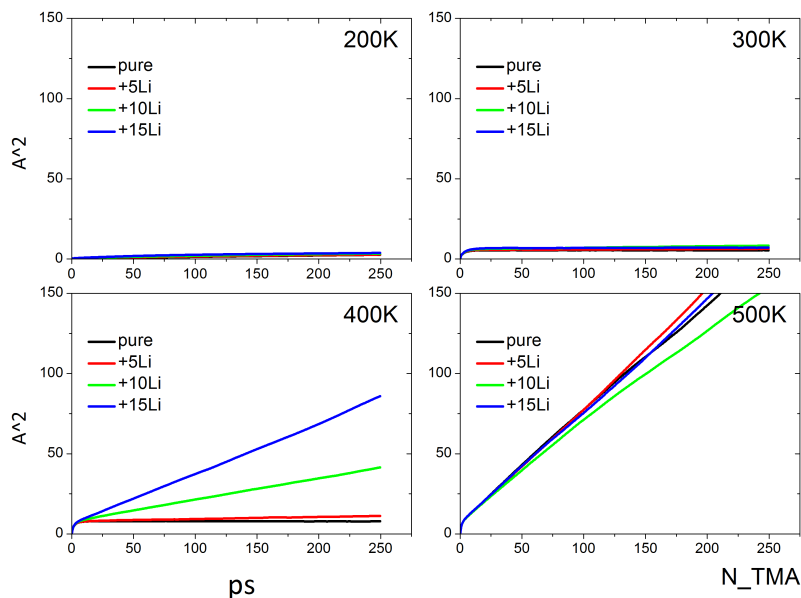


Figure S29: MSDs of central Nitrogens of [TMA]s vary as a function of lithium doping level within four temperature regimes (200 K, 300 K, 400 K and 500 K).

References

- (1) Smith, W.; Forester, T. R. DL_POLY_2.0: a general-purpose parallel molecular dynamics simulation package. *J Mol Graph* **1996**, *14*, 136–141.
- (2) C.W.Yong, DL_FIELD, STFC Daresbury Laboratory (2011). http://www.cse.scitech.ac.uk/ccg/software/DL_FIELD/.
- (3) Adebahr, J.; Grozema, F. C.; deLeeuw, S. W.; MacFarlane, D. R.; Forsyth, M. Structure and dynamics of the plastic crystal tetramethylammonium dicyanamide—a molecular dynamics study. *Solid State Ionics* **2006**, *177*, 2845–2850.
- (4) Peng, Z.; Ewig, C.; Hwang, M.; Waldman, M.; Hagler, A. Derivation of class ii force fields. 4. van der Waals parameters of Alkali metal cations and Halide anions. *The Journal of Physical Chemistry A* **1997**, *101*, 7243–7252.

- (5) Seeber, A. J.; Forsyth, M.; Forsyth, C. M.; Forsyth, S. A.; Annat, G.; MacFarlane, D. R. Conductivity, NMR and crystallographic study of N,N,N,N-tetramethylammonium dicyanamide plastic crystal phases: an archetypal ambient temperature plastic electrolyte material. *Phys. Chem. Chem. Phys.* **2003**, *5*, 2692.